31st Annual International Conference of the IEEE EMBS
Minneapolis, Minnesota, USA, September 2-6, 2009

3D Liver Segmentation in Preoperative CT Images using a Level-Sets Active Surface Method

Laura Fernández-de-Manuel, José L. Rubio, María J. Ledesma-Carbayo, Javier Pascau, José M. Tellado, Enrique Ramón, Manuel Desco, Andrés Santos

Abstract—**In this work we propose an active surface method to segment complete liver volumes from preoperative CT abdominal images. The method finds the surface that minimizes an energy function combining intensity inside and outside the surface, gradient information and curvature restrictions. The implementation is based on a level set technique following a multi-resolution strategy to reduce computing time. It requires only a single seed point inside the liver to initialize the active surface. The algorithm has been validated on a set of previously diagnosed livers. Resulting segmentations have been supervised by clinicians and radiologists, and numerically evaluated in terms of volume measurements with respect to those obtained from radiologists' manual segmentations. Additionally, radiologists analyzed the necessity of additional corrections on segmenting volumes.**

I. Introduction

HEPATIC surgery shows increasing complexity and precision thanks in part to the advances in the knowledge of the anatomy and hepatic physiology [1] as well as to the development of medical imaging techniques that allow preoperative planning [2]. Among the parameters essential for a safe liver surgery are the segmental location of the tumors, the relationship between tumors and the liver vasculature and the volume of the healthy functional liver, as well as the estimate of the remnant functional liver through surgery planning. Preoperative CT or MR studies enable an accurate staging and identification of the nature of the lesions, and are, so far, a mandatory source of liver imaging used by surgeons and radiologists for daily planning.

Traditionally, the hepatic segmentation has been carried out manually from preoperative CT images. Some current commercial systems offer tools with which the radiologist can manually segment 2D slices of the liver in transversal views. Since studies normally comprise from 100 to 500 slices, this procedure takes longer than 30 minutes, even when a sub-sampled version of the original CT is used.

Increasing the level of automation in the image segmentation process could save significant time and effort and enhance precision by eliminating human subjectivity.

The development of automatic and semiautomatic liver segmentation tools is particularly challenging due to its variability in size and shape and to the proximity to other organs of similar intensity value. Many works have been published in this field. Most of them are some variants of region growing [3] [4], level-sets or active contours [5] [6] [7], threshold classification or statistical analysis of the intensity distribution [8] [9], and statistical shape models or atlas [10] [11]. Methods based on the statistical analysis of the intensity distribution as well as statistical shape models require a huge quantity of training images and a priori knowledge about the shape and the size of the liver that could not be representative in damaged or resected livers.

In this work we propose a 3D active contour method based on level-sets specifically designed to segment the total functional liver in 3D CT abdominal images for a real clinical setting with the particular requirement of identifying only healthy parenchyma to assess liver function. The healthy parenchyma is considered as the region that includes only healthy tissue, excluding tumors and lesions taking into account radiologist's requirements in order to avoid overestimating the liver functional volume.

The proposed method is semi-automatic and requires only one seed point inside the liver to initialize the active surface.

The method has been evaluated in a set of seven previously diagnosed livers differing in size, shape and intensity. The obtained segmentations have been supervised and evaluated in terms of volume measurements and need of correction.

II. Proposed Method

The basic idea in active contour models is to evolve a contour subject to constraints from a given image. In the classical active contours models the curve evolves depending on the gradient of the image [12] [5]. Therefore, these models can detect only edges well defined by gradients. However, one of the problems when segmenting livers from CT images is the proximity to other organs of similar intensity that prevents from defining all the edges using only

Manuscript received June 17, 2009. This study was partially supported by research projects TIN 2007-68048-C02-01 and CDTEAM (CENIT) from the Spain's Ministry of Science.

Laura Fernández-de-Manuel, José L. Rubio, María J. Ledesma-Carbayo and Andrés Santos are with the Group of Biomedical Image Technologies, ETSIT, Universidad Politécnica de Madrid, Madrid 28040 Spain. and the CIBER BBN, Spain. {lfernandez, jlrubio, mledesma, andres}@die.upm.es

Javier Pascau and Manuel Desco are with "Medicina y Cirugía Experimental", Hospital General Universitario Gregorio Marañón, Madrid 28007 Spain.

José M. Tellado is with the "Servicio de Cirugía General I", Hospital General Universitario Gregorio Marañón, Madrid 28007 Spain.

Enrique Ramón is with the "Servicio de Radiodiagnóstico", Hospital General Universitario Gregorio Marañón, Madrid 28007 Spain.

gradient information.

In order to detect objects whose boundaries are not necessarily defined by a gradient, Chan et al. [13] proposed an active contour method based on the minimization of an energy function that depends both on image gray values inside and outside the curve at each iterative step (Mumford-Shah segmentation techniques [14]) and that is the departure point of our work:

$$F = \lambda_1 \int_{inside(C)} \left|u_0(x,y) - c_1\right|^2 dxdy + \lambda_2 \int_{outside(C)} \left|u_0(x,y) - c_2\right|^2 dxdy \quad (1)$$

where u_0 is a given image formed by two regions, C is an evolving contour, and the constants c_1 and c_2 depending on C are the averages of u_0 inside and outside C respectively.

This energy function can be formulated by level set techniques as described in [13]. The use of level set techniques for active contour implementations has become very popular, due to its ability of handling points presenting discontinuities and the possibility of topological changes. For the level set formulation the unknown variable C is replaced by the unknown variable ϕ, being ϕ a Lipschitz function:

$$\begin{aligned} &C = \partial\omega\{(x,y) \in \Omega : \phi(x,y) = 0\} \\ &inside(C) = \omega = \{(x,y) \in \Omega : \phi(x,y) < 0\} \\ &outside(C) = \Omega / \overline{\omega} = \{(x,y) \in \Omega : \phi(x,y) > 0\} \end{aligned} \quad (2)$$

The function (1) can be expressed using ϕ and the Heaviside H and Dirac δ_0 functions. The associated Euler – Lagrange equation for ϕ is deduced by minimizing the function with respect to ϕ. Finally, a linear system is obtained that can be solved by an iterative method (for more details we refer the reader to [13]):

$$\frac{\phi_{i,j}^{n+1} - \phi_{i,j}^{n}}{\Delta t} = \delta_h(\phi_{i,j}^{n}) \left[\mu \cdot div\left(\frac{\nabla \phi^n}{\left|\nabla \phi^n\right|}\right) - \gamma \right. \quad (3)$$
$$\left. + \lambda_1 (u_{0,i,j} - c_1(\phi^n))^2 - \lambda_2 (u_{0,i,j} - c_2(\phi^n))^2 \right]$$

where $\mu \geq 0$, $\gamma \geq 0$, λ_1, $\lambda_2 > 0$ are fixed parameters and Δt and h are the time and space steps respectively, used to discretize the equation in ϕ with a finite difference implicit scheme. The term $div(\nabla\phi^n / |\nabla\phi^n|)$ is used to restrict the curvature of the contour. Subscripts i, j represent the position.

However, this method works properly only with those images that contain two homogeneously well defined regions and textures. In the case of CT abdominal images, the liver region is homogeneous, but the outside of the liver is formed by several organs that can present both higher and lower intensities than the liver, and interfere with the good behavior of the described method [13]. Any of these intensities could be closer to the average gray value c_1 than to c_2, even when still differing considerably to c_1, a disparity that could be even bigger than the absolute difference between c_1 and c_2. This could erroneously lead to include those areas in the segmentation, which is not easily avoidable even by reducing the weight of the fourth term (λ_2).

In order to solve this problem we have introduced some variations to the function defined in Chan et al. [13], that allow segmenting a homogenous region (liver) that is adjacent to other organs with higher or lower intensities. For this reason the term that computes the difference between the gray value in a point and the average outside the contour is substituted by a term that computes the absolute difference between c_1 and c_2. The proposed active contour method combines the modified energy function based on gray values, with additional image gradient information in order to make the algorithm more robust. It has been implemented for 3D images, so we refer to it as active surface or 3D contour. The level sets function proposed in this article, that derives from equation (3), improves considerably the segmentation results with the images under study. The linear system proposed and solved iteratively, is the following:

$$\frac{\phi_{i,j,k}^{n+1} - \phi_{i,j,k}^{n}}{\Delta t} = \delta_h(\phi_{i,j,k}^{n}) \left[\mu \cdot div\left(\frac{\nabla \phi^n}{\left|\nabla \phi^n\right|}\right) - \gamma \right. \quad (4)$$
$$\left. + \lambda_1 \left|u_{0,i,j,k} - \rho \nabla u_{0,i,j,k} - c_1(\phi^n)\right| - \lambda_2 \left|c_1(\phi^n) - c_2(\phi^n)\right| \right]$$

where u_0 is a 3D image formed by two regions, one with almost constant intensity (liver), and the other one with different intensity organs. ϕ represents the evolving 3D contour. $\mu \geq 0$, $\gamma \geq 0$, ρ, λ_1, $\lambda_2 > 0$ are fixed parameters and Δt and h are the time and space steps respectively. The term $div(\nabla\phi^n / |\nabla\phi^n|)$ is used to restrict the curvature of the 3D contour or surface. In our calculations we fixed $\gamma = 0$, $\rho = 1$, $\lambda_1 = 1$ and $\lambda_2 = 1/5$ as they produce the best result. Only in cases of low contrast λ_2 should be smaller and ρ bigger.

The algorithm starts with a small surface obtained from a seed point placed inside the liver. The initial surface grows iteratively following the described linear system (4). The method has been implemented following a multi-resolution strategy in three pyramidal steps (Fig. 1) in order to reduce computing time because of the big size of CT abdominal images. In the first step, the resolution of the images is reduced to ¼ by means of bicubic interpolation. This fast initial segmentation allows us to select the liver region and to get a first approximate surface. In the second step, resolution is reduced to ½. At each step the growing surface begins with the previous step result and iterates more and more to the actual surface of the liver. Finally, in the last step, the resolution of the image is the original one and it performs a final growing of the previous surface that segments properly the liver.

The general active surface method is extended automatically with pre and post processing steps to address particular problems:

Case	Case description	Frontiers and Areas that needed correction	Volume from radiologist segmentation [cm^3]	Volume from proposed segmentation [cm^3]	Volume Diff.[%]	Time [s]
1	Hepatocarcinoma on cirrhotic liver	Heart, vena cava, left liver tip	2190	2227	+ 1.7	308
2	Recidivism in the left hemiliver after right hepatectomy	Heart, vena cava.	1050	935	-10.9	610
3	Liver metastasis undergoing portal vein embolization prior to mayor hepatic surgery	None	1336	1373	+2.8	379
4	Right hepatic lobule replaced by tumor	Heart and little areas	1421	1287	-9.4	489
5	Liver metastasis undergoing portal vein embolization prior to mayor hepatic surgery	Vena cava	1645	1560	-5.2	526
6	Liver metastasis	Vena cava	1000	1019	+1.9	247
7	Right hepatic lobule replaced by tumor	Stomach, pancreas.	1335	1340	+0.4	350

Table. 1. Cases descriptions, areas that needed corrections, volume measurements comparison and computation times.

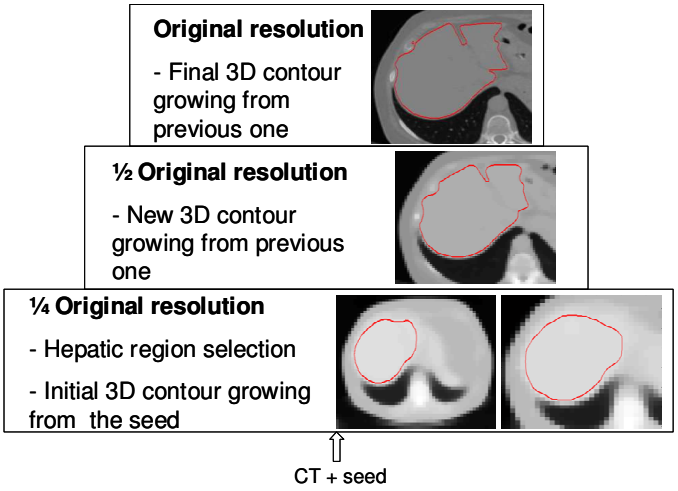

Fig. 1. Diagram of proposed pyramidal segmentation steps.

Pre-processing applied to the input CT images:

- Interpolation to make voxel sizes isotropic, thus facilitating the fitting of the surface evolution properties to the data.
- Median Filter to intensify the homogeneities.

Post-processing applied on the resulting segmentation:

- Morphological filtering to smooth the surface and to eliminate small unconnected zones. This filtering consists of a morphological erosion followed by a morphological reconstruction from the original seed point and a final morphological dilation.

III. Data and Validation

The proposed liver segmentation method has been validated on seven abdominal CT examinations (Table 1). The set was selected from a retrospective database of pathologic livers to include cases of different liver size and shapes, tumor intensities, and non-tumoral parenchyma textures. All studies were acquired with a Philips Brilliance 16 slice CT scanner except case 3 that was acquired on a Philips AV Expander multislice CT. The reference healthy liver volume was obtained from the pre-surgical radiologic report. The actual manual segmentations that derived from those measurements were not available.

The obtained segmentations have been evaluated by the radiologists supervising the results in terms of the total healthy liver included in the segmentation and the number of areas that needed correction. These areas were normally those adjacent to other organs or areas where radiologists would perform small modifications, for example, when vena cava is partially included (very difficult to segment even through visual inspection) or when the contour does not reach any of the sharpened liver tips. It is important to note that the inclusion or not of these small corrections does not affect significantly liver volume estimations. The numerical evaluation of our results has been made comparing the total functional liver volume reported (V_r) with respect to the measurement obtained with the proposed method (V_s) (Relative Volume Difference metric, *RVD*). The best value is 0 (for exact volumes) and the worst one is 100 or -100. The sign represents over segmentation (+) or infra segmentation (-).

$$RVD = \left((V_s - V_r)/V_r\right)\cdot 100 \qquad (5)$$

Volume measurements based on the obtained segmentations have been calculated using the spacing information of the CT slices and the pixel size.

IV. Results

The segmentations obtained with the proposed method were validated visually by the clinicians and the radiologists. Table 1 shows the described experiment results including case descriptions, the percentage of volume difference, areas that would need any correction after segmentation and the computation time for each examination. We can see that volume differences are, in all of the cases, smaller than 11%, reaching even values of 0.4 % (case 7). Case 2 presents the largest percentage of volume difference. This is due to the

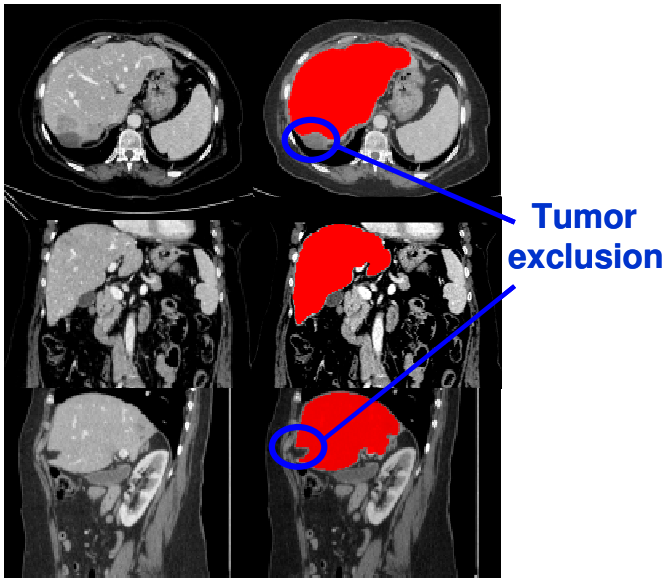

Fig. 2. Segmentation of healthy parenchyma in case 6. Top to bottom: transversal, coronal and sagittal slices.

small volume of the liver after hepatectomy. However, the visual supervision in case 2 showed a good behavior of the segmentation. Cases 4 and 7 presented special difficulties because of the big region with tumor. In case 4, inhomogeneities in the liver parenchyma produced mistakes in different small areas of the liver. The rest of the cases satisfied clinical requirements, even with very precise results (Fig, 2). Volume difference percentages were convenient. The areas that needed additional small correction in some cases were the heart, the vena cava, and the small tip of the left liver lobule (around segment II). However, this almost does not affect the final volume estimation because of its small size, and could be solved with the use of a few additional points that would imply restrictive forces in heart and vena cava areas. For that reason, clinicians warn of the necessity of an interface that allows them, in clinical practise, to modify or to correct certain details interactively. This point will be treated in future work.

Our method provides the results in 415 seconds (6.9 min) on average using a non optimized MATLAB code in one core of a PC at 2.4 GHz with 4 GB memory. It is important to note that the segmentation parameters were fixed except for case 4 that required a readjustment of λ_2 and ρ because of its atypical gray distribution.

Tumors have not been included in the liver selection, following the requirements of the clinicians. In this sense the proposed method works well, as it excludes hyperintense and hypointense tumors (Fig. 2).

V. Conclusion

In this work we propose an efficient 3D liver segmentation method based on active surface and level set techniques. It combines information from intensity, gradient and curvature restrictions. The method is implemented following a multi-resolution scheme and the only interaction needed is an initial seed point inside the liver. The method has been validated with a set of abdominal CT preoperative images, some of them with special difficulties, and it has demonstrated good performance. Further studies are guaranteed to correct the small areas that were misclassified. These corrections could be required in certain surgical planning applications even though the total amount of volume variation does not turn out to be of great relevance. Our method reduces the time needed in manual segmentations. Therefore, results seem promising, and consequently the proposed method is a valuable tool to estimate liver volumes in surgical planning.

References

[1] D. McClusky III, L. Skandalakis, G. Colborn, and J. Skandalakis, “Hepatic surgery and hepatic surgical anatomy: historical partners in progress”, *World Journal of Surgery*, vol. 21, no. 3, pp. 330-342, 1997.

[2] H. Handels and J. Ehrhardt, “Medical Image Computing for Computer-supported Diagnostics and Therapy. Advances and Perspectives”, *Methods of information in medicine*, vol. 48, no. 1, pp. 11-17, 2009.

[3] R. Pohle and K. D. Toennies, "Segmentation of medical images using adaptative region growing" *Proc. SPIE Medical Imaging*, vol. 2, no. 27, pp. 1337-1346, 2001.

[4] L. Ruskó, G. Bekes, G. Németh and M. Fridrich, "Fully automatic liver segmentation for contrast-enhanced CT images", *MICCAI Wshp. 3D Segmentation in the Clinic: A Grand Challenge*, pp. 143-150, 2007.

[5] V. Caselles, R. Kimmel and G. Sapiro, "Geodesic active contours", *International Journal of Computer Vision*, vol. 22, no. 1, pp. 61-79, 1997.

[6] G. Bekes, L. G. Nyül, E. Máté, A. Kuba and M. Fidrich. "3d segmentation of liver, kidneys and spleen from CT images" *Proc. International Journal of Conputer Assisted Radiology and Surgery*, vol. 2, no. 1, pp. 45-46, 2007

[7] J. Lee, N. Kim, H. Lee, J. B. Seo, H.J. Won,Y.M. Shin and Y. G. Shin, "Efficient Liver Segmentation exploiting Level-Set Speed Images with 2.5D Shape Propagation", *MICCAI Wshp. 3D Segmentation in the Clinic: A Grand Challenge*, pp. 189-196, 2007.

[8] S. J. Lim, Y. Y. Jeong and Y. S. Ho, "Automatic liver segmentation for volume measurement in CT Images", *J. Vis. Cmmun. Image R.*, vol. 17, no. 14, pp. 860-875, 2006

[9] L. Soler, H. Delingette, G. Malandain, J. Montagnat, N. Ayache, C. Koehl, O. Dourthe, B. Malassagne, M. Smith, D. Mutter, and J. Marescaux, "Fully automatic anatomical, pathological, and functional segmentation from CT scans for hepatic surgery", *Comput Aided Surg*, vol. 6, no. 3, pp. 131-142, 2001.

[10] D. Kainmueller, T. Lange and H. Lamecker, "ShapeConstrained Automatic Segmentation of the Liver based on Heuristic Intensity Model", *MICCAI Wshp. 3D Segmentation in the Clinic: A Grand Challenge*, pp. 109-116, 2007.

[11] H. Park, P. H. Bland and C. R. Meyer, "Construction of an Abdominal Probabilistic Atlas and its Application in Segmentation", *IEEE Trans. on Medical Imaging*, vol. 22, no. 4, pp. 483-492, April 2003.

[12] M. Kass, A. Witkin and D. Terzopoulos, "Snakes: Active Contour Models", *Int. J. Comput. Vis.* vol. 1, no. 4, pp 321-331, 1998.

[13] T. F. Chan and L. A. Vese, “Active Contours Without Edges”, *IEEE Trans. on Image Processing*, vol. 10, no. 2, pp. 266-277, February 2001.

[14] D. Mumford and J. Shah, “Optimal approximationsby piecewise smooth functions and associated variational problems”, *Cmmun. Pure Appl. Math*, vol. 42, no. 5, pp. 7-685, 1989.